

Superhydrophilic Graphene-Loaded TiO₂ Thin Film for Self-Cleaning Applications

Srinivasan Anandan,^{†,‡} Tata Narasinga Rao,[‡] Marappan Sathish,[§] Dinesh Rangappa,[§] Itaru Honma,[§] and Masahiro Miyauchi^{*,†,⊥}

[†]Department of Metallurgy and Ceramics Science, Graduate School of Science and Engineering, Tokyo Institute of Technology, 2-12-1 Ookayama, Meguro-ku, Tokyo 152-8552, Japan

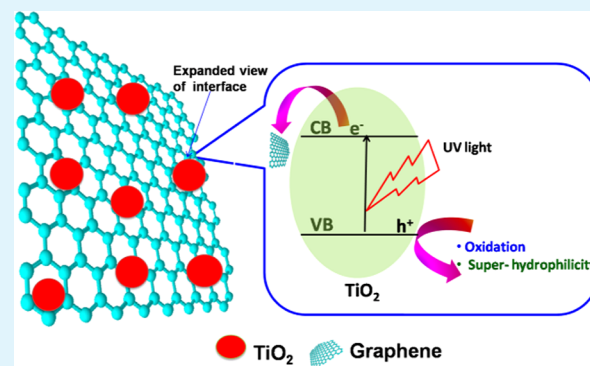
[‡]Centre for Nano Materials, International Advanced Research Center for Powder Metallurgy and New Materials, Balapur, Hyderabad 500 005, India

[§]Institute of Multidisciplinary Research for Advanced Materials, Tohoku University, 2-1-1, Katahira, Aoba-ku, Sendai 980-8577, Japan

[⊥]Japan Science and Technology Agency (JST), PRESTO, 4-1-8 Honcho Kawaguchi, Saitama 332-0012, Japan

ABSTRACT: We develop a simple approach to fabricate graphene-loaded TiO₂ thin films on glass substrates by the spin-coating technique. Our graphene-loaded TiO₂ films were highly conductive and transparent and showed enhanced photocatalytic activities. More significantly, graphene/TiO₂ films displayed superhydrophilicity within a short time even under a white fluorescent light bulb, as compared to a pure TiO₂ film. The enhanced photocatalytic activity of graphene/TiO₂ films is attributed to its efficient charge separation, owing to electrons injection from the conduction band of TiO₂ to graphene. The electroconductivity of the graphene-loaded TiO₂ thin film also contributes to the self-cleaning function by its antifouling effect against particulate contaminants. The present study reveals the ability of graphene as a low cost cocatalyst instead of expensive noble metals (Pt, Pd), and further shows its capability for the application of self-cleaning coatings with transparency. The promising characteristics of (inexpensive, transparent, conductive, superhydrophilic, and highly photocatalytically active) graphene-loaded TiO₂ films may have the potential use in various indoor applications.

KEYWORDS: graphene, TiO₂, photocatalytic oxidation, self-cleaning, superhydrophilicity



INTRODUCTION

Since graphene discovery in 2004, it has emerged as an outstanding material due to its unique properties,^{1–6} such as high electronic⁷ and thermal conductivity ($\sim 3000 \text{ W m}^{-1} \text{ K}^{-1}$),⁸ great mechanical strength ($\sim 1060 \text{ GPa}$),⁹ and high specific surface area ($\sim 2600 \text{ m}^2 \text{ g}^{-1}$).¹⁰ On the other hand, titanium dioxide (TiO₂) is a well-known wide-band gap semiconductor and has been investigated as an excellent photocatalyst, owing to its outstanding properties such as nontoxicity, low cost, and long-term stability.^{11,12} Because of unique characteristics, TiO₂ holds many possible applications including environmental and energy applications. TiO₂ is also used as an environmental cleanup material for antimicrobial and self-cleaning applications using photoenergy and rainwater. However, the photocatalytic efficiency of pure TiO₂ is quite limited, mainly due to rapid recombination of photogenerated electron–hole pairs within TiO₂ particles and lack of visible-light absorption. To overcome these limitations, several attempts such as loading of noble metal (Pt, Pd, and Au),¹³ cationic¹⁴ and anionic doping,^{15,16} sensitization,¹⁷ and addition of sacrificial reagents^{18–20} (electron and hole scavengers) have

been carried out. Pt loading on TiO₂ surface significantly increases the H₂ production²¹ efficiency by capturing the excited electrons from TiO₂. Further, electrons in noble metal particles such as Pt or Pd reduce oxygens into H₂O and H₂O₂ via two electrons or four electrons reduction, which paves the way to enhance charge separation between photogenerated electrons and holes.^{22–24} Though noble metals are good cocatalysts for the semiconductors, these cocatalysts are rare metals with high cost; thus, it is not appropriate for large scale applications. Hence, several research groups are trying to replace noble metal ions with low-cost additives for the development of highly efficient cost-effective photocatalysts. Graphene is a suitable alternative to noble metals because it has a high conductivity, high surface area, and the ability to favor the electron transfer from the conduction band of TiO₂ as graphene redox potential²⁵ is less negative than the conduction band edge of TiO₂. Hence, the photocatalytic applications of

Received: November 3, 2012

Accepted: December 15, 2012

Published: December 15, 2012

semiconductor–graphene composites have been extensively studied recently.^{26–37} It has been reported that decorating semiconductor materials with graphene can enhance their electronic,³⁸ optoelectronic,³⁹ electrocatalytic,⁴⁰ and photocatalytic properties. Most of the works reported to date on graphene–semiconductor systems are based on powder composite system. In contrast, thin film form is very important for practical application to utilize graphene characteristics like transparency and two-dimensional high electroconductivity. Recently, it was shown that graphene-oxide nanosheets on TiO₂ thin film used photoinactivation of bacteria.²⁷ However, no prior work regarding self-cleaning (superhydrophilic) applications of graphene based TiO₂ film has been reported, despite its significance in various applications. In recent years, the technology of self-cleaning surfaces has been developed rapidly with self-cleaning windows being the largest commercialization of self-cleaning coatings to date. The self-cleaning property has been known to be a mutual effect between photocatalysis and photoinduced hydrophilicity. The surface of TiO₂ displays photoinduced superhydrophilic conversion,⁴¹ and also, organic contaminants on the surface of TiO₂ can be removed by the photocatalytic oxidation reaction. Further, the surface electroconductivity is also very important to prevent adsorption of particulate contaminant by an antistatic effect. Therefore, three major qualities are mandatory for photocatalyst films to be applicable for self-cleaning. First, thin films must have a high photocatalytic activity, superhydrophilicity, and high durability. Second, the optical transparency is indispensable for the coating application like glass windows. Third, the electro-conductivity is very important to cause an antistatic property for retarding the adherence of the surface contaminants. By considering these issues, herein, we develop a simple strategy to fabricate a highly conductive and transparent graphene-loaded TiO₂ thin film. In the present work, we have investigated optical and electrical properties, photocatalytic oxidation activity, and superhydrophilic conversion for graphene/TiO₂ films. Photocatalytic reaction is expected to be enhanced by the loading of graphene, owing to the effective charge separation.

■ EXPERIMENTAL SECTION

Graphene sheets were prepared from graphite using the supercritical fluid method as reported previously.⁴² Initially, graphite crystals were placed in a stainless-steel reactor vessel and dispersed in ethanol using low power sonication for 10 min. Then, the reactor was sealed and heated to 300–400 °C for 30 min. Finally, the reactor vessel was immersed in an ice-cold bath to stop the reaction inside the vessel. Exfoliated graphene sheets were obtained by washing and centrifuging the reaction mixture by ethanol repeatedly, which is followed by vacuum-drying at 100 °C overnight. The resulting graphene sheets were used for the preparation of graphene-loaded TiO₂ films. The amount of graphene and TiO₂ in graphene/TiO₂ film is 5 wt % and 95 wt %, respectively. In order to achieve this ratio, we have used 3.6 g of titanium(IV) bis ammonium lactate dihydroxide (equivalent to ~0.95 g of TiO₂) and 0.05 g of graphene sheets for the fabrication of graphene/TiO₂ film. Glass substrates were used to prepare films. Before coating, the glass substrates were ultrasonically degreased in ethanol and were then thoroughly rinsed with distilled water. Graphene/TiO₂ films were prepared by the spin-coating process. Titanium(IV) bis ammonium lactate dihydroxide (TBLAH) was used as the TiO₂ source. TBLAH was mixed with 10 mL of water (H₂O), and the resulting mixture was added to the required amount of graphene sheets. Then, the dispersions were sonicated vigorously for complete dispersion of graphene. Glycerol was added to the above dispersions to prepare homogeneous graphene/TiO₂ films. The

graphene dispersed TBLAH solution was spin-coated on glass substrates and dried at 100 °C for 1 h. Then, the above synthesized films were annealed at 400 °C for 2 h. For comparison, TiO₂ films were prepared by the same procedures without adding graphene sheets. Powder samples of TiO₂ and graphene-loaded TiO₂, obtained from the same solution for thin film synthesis, were characterized by X-ray diffraction, scanning electron microscope (SEM), and transmission electron microscope (TEM) analysis. The crystal phases were evaluated by X-ray diffraction with Cu K α X-rays (XRD model Ultima-3, Rigaku Co., Tokyo, Japan). The XRD patterns of graphene/TiO₂ films were measured by a grazing angle method. In this method, the incident angle was fixed at 0.5° and 2θ was scanned in the range from 20° to 80°. The morphology of the prepared samples was observed using a Hitachi S-4800 field emission scanning electron microscope (FE-SEM, Hitachi Co. Ltd. S-4800). Scanning and high resolution transmission electron micrographs were recorded with a JEOL JEM-2100F microscope, working at an accelerating voltage of 200 kV. The transmittance of thin films was measured using a spectrophotometer (UV-2100, Shimadzu Co., Kyoto, Japan). The sheet resistance of the samples was measured by a four pin probe resistivity meter (Loresta GP, Mitsubishi Chemical Co) as reported earlier.⁴³

The surface wettability related to self-cleaning properties was evaluated by the water contact angle. The measurements were performed at room temperature using a commercial contact angle meter (DM-500, Kyowa Interface Science, Saitama, Japan). High purity water was used for all measurements. Contact angle measurements were conducted on three points for each sample, and the experimental error for each point was within ± 1 degree. Light illumination was provided by a white fluorescent light bulb. The light intensity measured by a UV radiometer (USR-45D, Ushio Co.) was 20 $\mu\text{W cm}^{-2}$. The photocatalytic activities of the graphene/TiO₂ thin films were evaluated by the degradation of methylene blue (MB) with a concentration of 0.01 mM in an aqueous solution. UV-light irradiation was provided by a 40 W cylindrical black light bulb (Toshiba Co, Tokyo, Japan) with an intensity of 1.5 mW cm^{-2} , which was determined by a UV radiometer (USR-45D, Ushio Co.). Graphene/TiO₂ film was immersed in 3 mL of MB solution and kept in the dark for 1 h to reach the adsorption–desorption equilibrium before irradiation. The distance of the quartz cell and the UV light source was maintained at 5 cm. At a certain time interval during the experiment, absorbance values of MB solution were measured by a spectrophotometer (UV-2100, Shimadzu Co., Kyoto, Japan). Before each absorbance measurement, thin films were stored in the dark for 2 h to reconvert the reduced methylene blue of the leuco form (LMB) into its initial state.⁴⁴ With this procedure, changes in absorbance values can be ascribed to the level of MB decomposition from the oxidation reaction. The peak absorbance value of MB appeared at 664 nm, and the change of absorbance was measured at the peak value on a spectrophotometer. For comparison, the photocatalytic activity of the pure TiO₂ films was also evaluated under the same experimental conditions.

■ RESULTS AND DISCUSSION

The crystallinity of the samples was measured by the X-ray diffraction pattern, and the results are shown in Figure 1A. The XRD pattern (a in Figure 1A) at $2\theta = 26.35^\circ$ corresponds to (002) reflection, confirming the presence of graphene. The peak at $2\theta = 24^\circ$ corresponds to restacking^{45a} of the graphene nanosheets during the reduction process of graphene oxide. The XRD diffraction at $2\theta = 26.35^\circ$, in the present study, is due to the presence of exfoliated graphene obtained from graphite by the super critical fluid method, which indexes to the (002) planes of hexagonal graphite (JCPDS card No. 41-1487).^{45b} The results are consistent with the XRD patterns reported previously.⁴⁵ When graphene is loaded with TiO₂, the diffraction pattern (b in Figure 1A) of anatase TiO₂ appeared in addition to graphene peaks. The peaks observed at $2\theta = 25.1^\circ$ (101), 37.6° (004), 47.7° (200), 53.8° (105), 54.6°

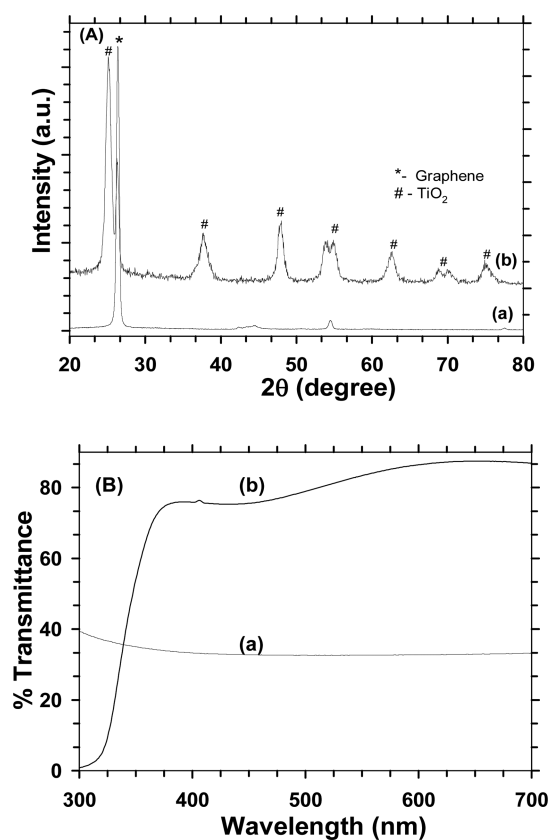


Figure 1. X-ray diffraction pattern (A) and UV-vis spectrum (B) of graphene (a) and graphene-loaded TiO₂ films (b).

(211), 62.5° (204), 68.6° (116), 69.8° (220), and 74.75° (215) are assigned to anatase titanium dioxide.⁴⁶ UV-vis spectra for graphene and graphene/TiO₂ thin films are shown in Figure 1B. Graphene shows a broad spectrum in the entire wavelength region, while graphene-loaded TiO₂ exhibit a typical UV-vis spectrum of TiO₂. Transmittance was decreased around the UV region, owing to the absorption by the band gap excitation of TiO₂. The thicknesses of graphene and graphene/TiO₂ films were nearly identical for the study of UV-vis absorption, but the graphene/TiO₂ was optically transparent, since a small amount of graphene was used for this film. A high resolution transmission electron microscopy (HR-TEM) image of graphene and graphene/TiO₂ reveals that graphene exists as a few single layers of a graphene sheet (Figure 2a), and TiO₂ particles are uniformly dispersed on graphene sheets (Figure 2b).

Electroconductivity is very important for antifouling of charged dust particles. High electroconductivity surface with antistaticity properties retard the adsorption of charged contaminant particles. For example, indium tin oxide (ITO) is used for antifouling agent⁴⁷ due to its excellent electron conductivity. The sheet resistance results are shown in Figure 3. The resistance values of TiO₂, graphene, and graphene-loaded TiO₂ films were 1.8, 0.3, and 0.4 ohms per square, respectively. When graphene was loaded with TiO₂, its resistivity was very close to the pure graphene film, while that of the pure TiO₂ film was much higher than the graphene-loaded TiO₂ films. The thickness of single layer TiO₂ film, measured by SEM cross section analysis, was ~70 nm, which was nearly identical with those of the graphene-loaded TiO₂ films. Although our

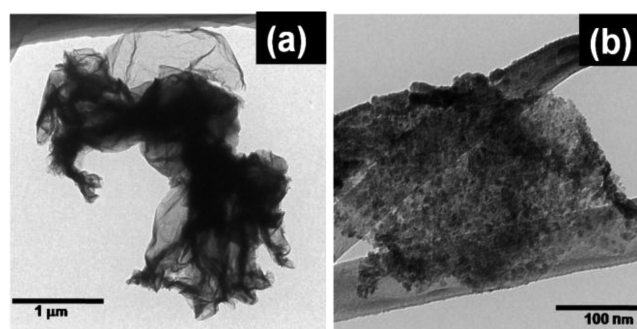


Figure 2. HR-TEM images of graphene sheet (a) and graphene-loaded TiO₂ (b).

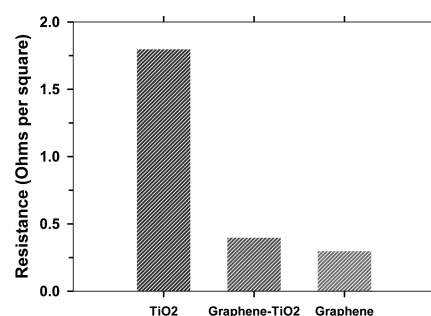


Figure 3. Resistivity values of TiO₂, graphene, and graphene-loaded TiO₂ thin films.

graphene/TiO₂ film exhibited significant electroconductivity, it was visibly transparent as shown in our UV-vis spectrum.

The photocatalytic decomposition of MB solution under UV irradiation is shown in Figure 4. Figure 4A shows the results for pure TiO₂ thin films with different thicknesses. The numerical values 1, 3, 5, 7, and 10 indicate the number of spin-coating of TiO₂ on glass substrate. When TiO₂ layer increases, the decomposition of methylene blue also increases and reaches maximum decomposition efficiency at three layers (thickness ~ 100 nm) of TiO₂. MB solution (80%) decomposed within 36 h of irradiation time by three layers of TiO₂ films. Further increase in TiO₂ layers resulted in a decrease of photocatalytic activity. Figure 4B shows the results of MB decomposition using graphene-loaded TiO₂ films. When graphene is added over TiO₂, the photocatalytic activity was further enhanced and exhibited complete decomposition of MB. It was found that three layers of TiO₂-loaded graphene films require 18 h of irradiation time for complete decoloration of MB solutions. The photocatalytic efficiency of graphene-loaded TiO₂ films is about 2-fold higher than pure TiO₂ films. At higher graphene loading, the decomposition of MB decreases. This observation can be explained by the fact that an increase in film thickness can restrain the light penetration due to the shadowing effect of graphene. Initial concentrations of MB in the dark condition were nearly the same for pure TiO₂ and graphene/TiO₂, indicating that the adsorbabilities for these films were nearly identical in the present study, and our MB decomposition reaction has been conducted under light-limited conditions, in which the reaction rate strongly depends on the electron-hole charge separation efficiency.⁴⁸ Therefore, the enhancement in photocatalytic activity is mainly due to the electron transfer from TiO₂ to graphene.

Next, we investigated the self-cleaning property in the indoor environment since water contact angle has strong relation with

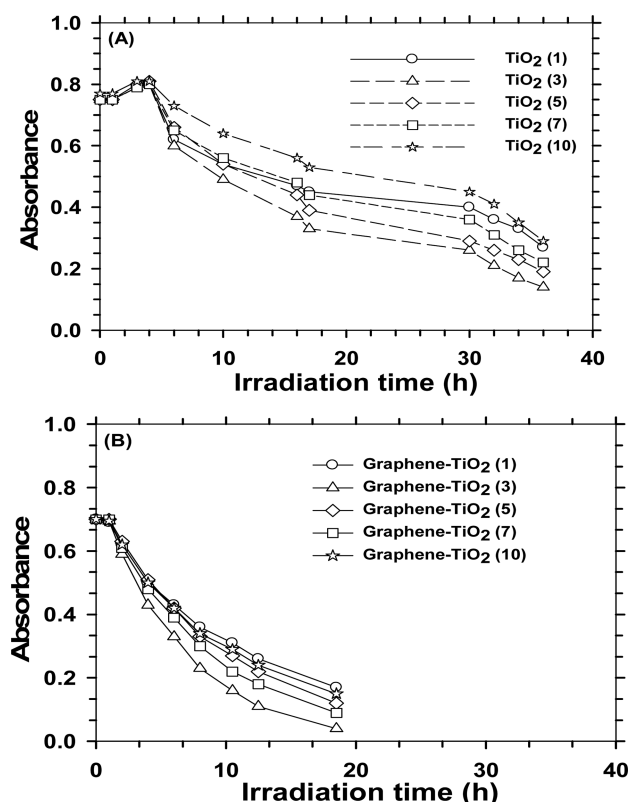


Figure 4. UV-light induced photocatalytic oxidation of methylene blue (MB) using TiO_2 and graphene-loaded TiO_2 thin films. Change in absorbance spectrum of MB as a function of irradiation time using TiO_2 (A) and graphene-loaded TiO_2 films (B). The numerical values 1, 3, 5, 7, and 10 indicate the number of layers of TiO_2 and graphene/ TiO_2 on glass substrate. (Photocatalytic reaction conditions: concentration of MB = 0.01Mm (3 mL); light source = black light; light intensity = 5 mw/cm².)

self-cleaning properties.^{41b} Figure 5 shows the results of surface wettability of various films. The water contact angles of the

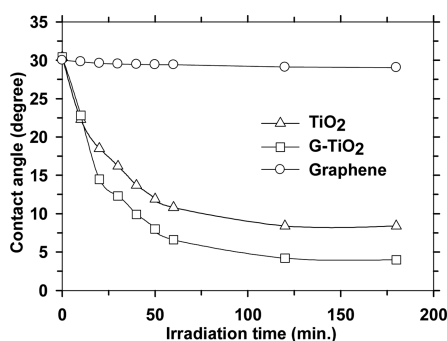


Figure 5. Changes in water contact angle under UV-light irradiation using TiO_2 and graphene-loaded TiO_2 films. (Photocatalytic reaction conditions: light source = fluorescent white bulb; light intensity = 20 $\mu\text{w}/\text{cm}^2$.)

graphene film did not decrease even after long irradiation time since it is photocatalytically inactive. In contrast, the water contact angles of pure TiO_2 and graphene TiO_2 films gradually decreased with increasing irradiation time. It is noted that hydrophilic conversion rate of the graphene/ TiO_2 film is higher than that of the pure TiO_2 film. Our films were not active under visible light with the UV cutting off filter, indicating that the

hydrophilic reaction was induced by UV light, which was irradiated from a white fluorescent light bulb. Photoinduced hydrophilic conversion originates from the oxidation of surface contaminants as well as the structural changes of TiO_2 surface.⁴¹ Both the decomposition of surface contaminants and photoinduced surface structural changes require high oxidation power of photogenerated holes in the valence band of TiO_2 .⁴⁹ Our group^{50,51} has reported the noble metal cocatalysts like Pt or Pd accelerate the photoinduced superhydrophilicity of metal oxide semiconductors. As an alternative to noble metals, in the present study, we successfully fabricated superhydrophilic TiO_2 using inexpensive graphene as cocatalyst. Graphene acts as electron sink,⁵² similar to noble metals, but the graphene film is optically transparent as compared to composites of noble metal and metal oxide particles. Further, the graphene has a sheetlike structure, and its sheet resistance is much lower than those of noble metal and metal oxide composites.

The charge transfer mechanism that occurs in the graphene/ TiO_2 film during photocatalytic oxidation is shown in Figure 6.

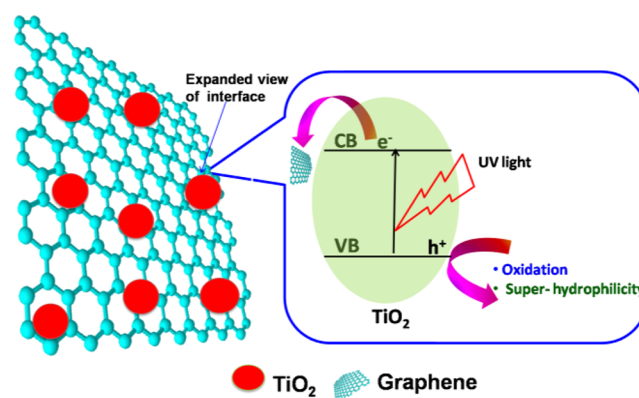


Figure 6. Charge transfer mechanism in graphene/ TiO_2 thin film during photocatalytic reaction.

When UV light is irradiated on the TiO_2 surface, it generates holes and electrons. In pure TiO_2 films, electrons and holes quickly recombine, resulting in low reactivity. In contrast, when TiO_2 is loaded with graphene, the electrons transfer (see Figure 6) to graphene, since the potential (−0.08 V vs. standard hydrogen electrode (SHE), pH = 7) of graphene/graphene• lies below the conduction band (−0.4 V vs. SHE, pH = 7⁵³) of TiO_2 . The graphene sheet promotes the effective charge separation for photogenerated electrons and holes.^{52,54,55} The photogenerated holes in the valence bond (VB) of TiO_2 used for the oxidation of MB solution. Moreover, holes in TiO_2 react with surface lattice oxygen atoms, which is followed by the dissociative adsorption of a water molecule, making the surface become superhydrophilic. Graphene loading with TiO_2 is efficient to enhance the charge separation of holes and electrons. Due to these holes and electron transfers, charge recombination is suppressed in TiO_2 films and hence largely enhances the efficiency of photocatalytic oxidation and self-cleaning properties.

CONCLUSION

Optically transparent and highly electroconductive graphene/ TiO_2 film has been developed by a facile fabrication method. Graphene/ TiO_2 film shows enhanced photocatalytic activity under UV light irradiation. The photocatalytic efficiency of

graphene/TiO₂ film is 2-fold higher than TiO₂ film alone. Moreover, the graphene/TiO₂ film surface exhibits superhydrophilic properties within a short time compared to TiO₂ film. Efficient charge separation in TiO₂ by electron transfer from a conduction band of TiO₂ to graphene is attributed to the enhanced photocatalytic oxidation and photoinduced superhydrophilicity. The present study first reports the graphene/TiO₂ thin film with transparency, electroconductivity, highly photocatalytic oxidation, and photoinduced superhydrophilic properties, and the developed technique is very useful for the application of self-cleaning coating, especially under the extremely low UV intensity like indoor light apparatus, such as a white fluorescent light bulb.

AUTHOR INFORMATION

Corresponding Author

*E-mail: mmiyauchi@ceram.titech.ac.jp.

Notes

The authors declare no competing financial interest.

ACKNOWLEDGMENTS

We thank the Japan Society for Promotion of Science (JSPS) to provide a fellowship and a research grant through the Ministry of Education, Culture, Sports, Science and Technology of Japan (MEXT). This research was also supported by JST, PREST.

REFERENCES

- (1) Novoselov, K. S.; Geim, A. K.; Morozov, S. V.; Jiang, D.; Zhang, Y.; Dubonos, S. V.; Grigorieva, I. V.; Firsov, A. A. *Science* **2004**, *306*, 666–669.
- (2) Geim, A. K.; Novoselov, K. S. *Nat. Mater.* **2007**, *6*, 183–191.
- (3) Li, D.; Kaner, R. B. *Science* **2008**, *320*, 1170–1171.
- (4) Rao, C. N. R.; Sood, A. K.; Subrahmanyam, K. S.; Govindaraj, A. *Angew. Chem., Int. Ed.* **2009**, *48*, 7752–7777.
- (5) Geim, A. K. *Science* **2009**, *324*, 1530–1534.
- (6) Park, S.; Ruoff, R. S. *Nat. Nanotechnol.* **2009**, *4*, 217–224.
- (7) Du, X.; Skachko, I.; Barker, A.; Andrei, E. Y. *Nat. Nanotechnol.* **2008**, *3*, 491–495.
- (8) Balandin, A. A.; Ghosh, S.; Bao, W. Z.; Calizo, I.; Teweldebrhan, D.; Miao, F.; Lau, C. N. *Nano Lett.* **2008**, *8*, 902–907.
- (9) Lee, C.; Wei, X. D.; Kysar, J. W.; Hone, J. *Science* **2008**, *321*, 385–388.
- (10) Schniepp, H. C.; Li, J. L.; McAllister, M. J.; Sai, H.; Herrera-Alonso, M.; Adamson, D. H.; Prud'homme, R. K.; Car, R.; Saville, D. A.; Aksay, I. A. *J. Phys. Chem. B* **2006**, *110*, 8535–8539.
- (11) Linsebigler, A. L.; Lu, G. Q.; Yates, J. T. *Chem. Rev.* **1995**, *95*, 735–758.
- (12) Fujishima, A.; Hashimoto, K.; Watanabe, T. *TiO₂ Photocatalysis, Fundamentals and Applications*; BKC, Inc.: Tokyo, 1999.
- (13) Sakthivel, S.; Shankar, M. V.; Palanichamy, M.; Arabindoo, B.; Bahnemann, D. W.; Murugesan, V. *Water Res.* **2004**, *38*, 3001–3008.
- (14) Highfield, J. G.; Pichat, P. *New J. Chem.* **1989**, *13*, 61–66.
- (15) Asahi, R.; Morikawa, T.; Ohwaki, T.; Aoki, K.; Taga, Y. *Science* **2001**, *293*, 269–271.
- (16) Sakthivel, S.; Kisch, H. *Angew. Chem., Int. Ed.* **2003**, *42*, 4908–4911.
- (17) Jin, Z. L.; Zhang, X. J.; Li, Y. X.; Li, S. B.; Lu, G. X. *Catal. Commun.* **2007**, *8*, 1267.
- (18) Zielinska, B.; Borowiak-Palen, E.; Kalenczuk, R. J. *Int. J. Hydrogen Energy* **2008**, *33*, 1797.
- (19) Yang, X. H.; Li, Z.; Liu, G.; Xing, J.; Sun, C. H.; Yang, H. G.; Li, C. Z. *CrystEngComm* **2011**, *13*, 1378.
- (20) Liu, G.; Yang, H. G.; Wang, X. W.; Cheng, L. N.; Pan, J.; Lu, G. Q.; Cheng, H. M. *J. Am. Chem. Soc.* **2009**, *131*, 12868.
- (21) (a) Hufschmidt, D.; Bahnemann, D.; Testa, J. J.; Emilio, C. A.; Litter, M. I. *J. Photochem. Photobiol., A* **2002**, *148*, 223–231. (b) Yang, Y. Z.; Chang, C.-H.; Idriss, H. *Appl. Catal., B* **2006**, *67*, 217–222. (c) Patsoura, A.; Kondarides, D. I.; Vekyrios, X. E. *Appl. Catal., B* **2006**, *64*, 171–179.
- (22) Abe, R.; Takami, H.; Murakami, N.; Ohtani, B. *J. Am. Chem. Soc.* **2008**, *130*, 7780–7781.
- (23) Zhao, Z. G.; Miyauchi, M. *Angew. Chem., Int. Ed.* **2008**, *47*, 7051–7055.
- (24) Arai, T.; Horiguchi, M.; Yanagida, M.; Gunji, T.; Sugihara, H.; Sayama, K. *Chem. Commun.* **2008**, 5565–5567.
- (25) Xiang, Q.; Yu, J.; Jaroniec, M. *J. Am. Chem. Soc.* **2012**, *134*, 6575–6578.
- (26) Williams, G.; Seger, B.; Kamat, P. V. *ACS Nano* **2008**, *2*, 1487–1491.
- (27) Akhavan, O.; Ghaderi, E. *J. Phys. Chem. C* **2009**, *113*, 20214–20220.
- (28) Zhang, Y.; Tang, Z.-R.; Fu, X.; Xu, Y. *ACS Nano* **2010**, *4*, 7303–7314.
- (29) Zhang, H.; Lv, X. J.; Li, Y. M.; Wang, Y.; Li, J. H. *ACS Nano* **2010**, *4*, 380–386.
- (30) Zhang, X. Y.; Li, H. P.; Cui, X. L.; Lin, Y. J. *Mater. Chem.* **2010**, *20*, 2801–2086.
- (31) Chen, C.; Cai, W.; Long, M.; Zhou, B.; Wu, Y.; Wu, D.; Feng, Y. *ACS Nano* **2010**, *4*, 6425–6432.
- (32) Zhang, Y.; Tang, Z.-R.; Fu, X.; Xu, Y. *ACS Nano* **2011**, *5*, 7426–7435.
- (33) Zhou, K.; Zhu, Y.; Yang, X.; Jiang, X.; Li, C. *New J. Chem.* **2011**, *35*, 353–359.
- (34) Zhang, Y.; Pan, C. *J. Mater. Sci.* **2011**, *46*, 2622–2626.
- (35) Fan, W.; Lai, Q.; Zhang, Q.; Wang, Y. *J. Phys. Chem. C* **2011**, *115*, 10694–10701.
- (36) Guo, J.; Zhu, S.; Chen, Z.; Li, Y.; Yu, Z.; Liu, Q.; Li, J.; Feng, C.; Zhang, D. *Ultrason. Sonochem.* **2011**, *18*, 1082–1090.
- (37) Xu, T.; Zhang, L.; Cheng, H.; Zhu, Y. S. *Appl. Catal., B* **2011**, *101*, 382–387.
- (38) Wang, D. H.; Choi, D. W.; Li, J.; Yang, Z. G.; Nie, Z. M.; Kou, R.; Hu, D. H.; Wang, C. M.; Saraf, L. V.; Zhang, J. G.; Aksay, I. A.; Liu, J. *ACS Nano* **2009**, *3*, 907.
- (39) Cao, A. N.; Liu, Z.; Chu, S. S.; Wu, M. H.; Ye, Z. M.; Cai, Z. W.; Chang, Y. L.; Wang, S. F.; Gong, Q. H.; Liu, Y. F. *Adv. Mater.* **2010**, *22*, 103.
- (40) Ng, Y. H.; Iwase, A.; Kudo, A.; Amal, R. *J. Phys. Chem. Lett.* **2010**, *1*, 2607.
- (41) (a) Wang, R.; Hashimoto, K.; Fujishima, A.; Chikuni, M.; Kojima, E.; Kitamura, A.; Shimohigoshi, M.; Watanabe, T. *Nature* **1997**, *388*, 431–432. (b) Wang, R.; Hashimoto, K.; Fujishima, A.; Chikuni, M.; Kojima, E.; Kitamura, A.; Shimohigoshi, M.; Watanabe, T. *Adv. Mater.* **1998**, *10*, 135–138.
- (42) Rangappa, D.; Sone, K.; Wang, M.; Gautam, U. K.; Golberg, D.; Itoh, H.; Ichihara, M.; Honam, I. *Chem.—Eur. J.* **2010**, *16*, 6488.
- (43) Li, Y.; Shimizu, H. *Macromolecules* **2009**, *42*, 2587.
- (44) (a) Miyauchi, M.; Nakajima, A.; Fujishima, A.; Hashimoto, K.; Watanabe, T. *Chem. Mater.* **2000**, *12*, 3–5. (b) Miyauchi, M.; Nakajima, A.; Watanabe, T.; Hashimoto, K. *Chem. Mater.* **2002**, *14*, 2812–2816. (c) Miyauchi, M.; Nakajima, A.; Watanabe, T.; Hashimoto, K. *Chem. Mater.* **2002**, *14*, 4714–4720. (d) Mills, A.; Wang, J. J. *Photochem. Photobiol., A: Chem.* **1999**, *127*, 123–134.
- (45) (a) Li, M.; Huang, X.; Wu, C.; Xu, H.; Jiang, P.; Tanaka, T. *J. Mater. Chem.* **2012**, *22*, 23477–23484. (b) Qian, W.; Chen, Z.; Eastman, M.; Cottingham, S.; Manhat, B. A.; Goforth, A.; Jiao, J. *Ultramicroscopy* **2012**, *119*, 97–101. (c) Wang, G.; Yang, J.; Park, J.; Gou, X.; Wang, B.; Liu, H.; Yao, J. *J. Phys. Chem., C* **2008**, *112*, 8192.
- (46) Sivalingam, G.; Nagaveni, K.; Hedge, M. S.; Madras, G. *Appl. Catal., B: Environ.* **2003**, *45*, 23.
- (47) Shiddiky, M. J.A.; Kithva, P. H.; Rauf, S.; Trau, M. *Chem. Commun.* **2012**, *48*, 6411–6413.
- (48) Ohko, Y.; Hashimoto, K.; Fujishima, A. *J. Phys. Chem. A* **1997**, *101*, 8057–8062.
- (49) Sakai, N.; Fujishima, A.; Watanabe, T.; Hashimoto, K. *J. Phys. Chem., B* **2003**, *107*, 1028–1035.

- (50) Miyauchi, M. *Phys. Chem. Chem. Phys.* **2008**, *10*, 6258.
- (51) Shibuya, M.; Miyauchi, M. *Adv. Mater.* **2009**, *21*, 1373.
- (52) Xiang, Q.; Yu, J.; Jaroniec, M. *Nanoscale* **2011**, *3*, 3670.
- (53) Paola, A. D.; Bellardita, M.; Palmisano, L. *Stud. Surf. Sci. Catal.* **2010**, *175*, 225–228.
- (54) Li, Q.; Guo, B. D.; Yu, J. G.; Ran, J. R.; Zhang, B. H.; Yan, H. J.; Gong, J. R. *J. Am. Chem. Soc.* **2011**, *133*, 10878.
- (55) Wang, X.; Zhi, L. J.; Mullen, K. *Nano Lett.* **2008**, *8*, 323.